Scientific paper

Surface Passivation of Natural Graphite Electrode for Lithium Ion Battery by Chlorine Gas

Satoshi Suzuki,[1] Zoran Mazej,[2] Boris Žemva,[2] Yoshimi Ohzawa[1] and Tsuyoshi Nakajima[1,*]

[1] *Department of Applied Chemistry, Aichi Institute of Technology, Yakusa, Toyota 470-0392, Japan*

[2] *Jožef Stefan Institute, 39 Jamova, 1000 Ljubljana, Slovenia*

* *Corresponding author: E-mail: nakajima-san@aitech.ac.jp*
Tel.: +81 565 488121; fax: +81 565 480076.

Received: 28-06-2012

Dedicated to Prof. Dr. Boris Žemva on the occasion of receiving the Zois´ award for lifetime achievements.

Abstract

Surface lattice defects would act as active sites for electrochemical reduction of propylene carbonate (PC) as a solvent for lithium ion battery. Effect of surface chlorination of natural graphite powder has been investigated to improve charge/discharge characteristics of natural graphite electrode in PC-containing electrolyte solution. Chlorination of natural graphite increases not only surface chlorine but also surface oxygen, both of which would contribute to the decrease in surface lattice defects. It has been found that surface-chlorinated natural graphite samples with surface chlorine concentrations of 0.5–2.3 at% effectively suppress the electrochemical decomposition of PC, highly reducing irreversible capacities, i.e. increasing first coulombic efficiencies by 20–30% in 1 molL^{-1} $LiClO_4$–EC/DEC/PC (1:1:1 vol.). In 1 molL^{-1} $LiPF_6$–EC/EMC/PC (1:1:1 vol.), the effect of surface chlorination is observed at a higher current density. This would be attributed to decrease in surface lattice defects of natural graphite powder by the formation of covalent C–Cl and C=O bonds.

Keywords: Surface modification, chlorine gas, chlorination, natural graphite electrode, lithium ion battery

1. Introduction

Lithium ion batteries using ethylene carbonate (EC)-based solvents have a disadvantage on the low temperature operation because EC has a high melting point of 36 °C. For natural graphite anode with high crystallinity, EC should be used for the quick formation of surface film (Solid Electrolyte Interphase: SEI) by decomposition of a small amount of solvent. To improve the low temperature operation of lithium ion batteries, it is desirable to use propylene carbonate (PC) with a low melting point, –55 °C. However, it is difficult to use PC for natural graphite with high crystallinity because electrochemical reduction continues on natural graphite surface without forming surface film, which gives a large irreversible capacity. Natural graphite powder is prepared by mechanical pulverizing of large particles. Therefore many lattice defects would exist at the surface, functioning as active sites for electrochemical reduction of the solvents. Various methods of surface modification have been applied to improve electrode characteristics of carbonaceous anodes for lithium ion batteries. They are carbon coating,[1–14] metal or metal oxide coating,[15–25] surface oxidation,[26–33] surface fluorination[34–50] and polymer, Si or Sb coating.[51–58] These methods of surface modification improved the electrochemical properties of carbonaceous electrodes for lithium ion batteries. Surface fluorination using fluorinating gases such as F_2 and ClF_3 and plasma fluorination are effective for improving charge/discharge properties of natural and synthetic graphites. Surface fluorination of graphitized petroleum cokes opens closed edge surface and enhances surface disorder, which facilitates the formation of surface film on graphite, leading to increase in first coulombic efficiencies (decrease in irreversible capacities).[38–40, 43–46] Surface fluorination of natural graphite powder samples with relatively small surface areas (< 5 m^{2}g^{-1}) increases the capacities by increasing surface areas and surface disorder.[34–37,41] On the other hand, main effect of surface

fluorination of those having large surface areas (7–14 m^2g^{-1}) is the surface passivation by forming covalent C–F bonds at the surface, which suppresses electrochemical reduction of PC, increasing first coulombic efficiencies of natural graphite in PC-containing solvents.[42,47–50] Since F_2 has a small dissociation energy (155 $kJmol^{-1}$) and highest electronegativity, F_2 has high reactivity with other simple substances and compounds. Even light fluorination using F_2 causes the increase in surface area and surface disordering of graphite with formation of covalent C–F bonds. However, Cl_2 gas has lower reactivity than F_2 because of its larger dissociation energy (239 $kJmol^{-1}$) and lower electronegativity. Therefore it is expected that chlorination of natural graphite powder by Cl_2 gas yields covalent C–Cl bonds at the surface without increase in surface area and surface disorder. In the present study, surface passivation of natural graphite powder samples has been performed using Cl_2 gas and electrochemical behavior of surface-chlorinated samples has been investigated in PC-containing electrolyte solutions.

2. Experimental

2. 1. Surface Chlorination and Analyses of Natural Graphite Samples

Natural graphite powder samples with average particle sizes of 10 and 15 μm (abbreviated to NG10 μm and NG15 μm; d_{002} = 0.335 and 0.336 nm; surface area:[47] 9.2 and 6.9 m^2g^{-1}, respectively; purity: >99.95%), supplied by SEC Carbon Co., Ltd., were chlorinated by Cl_2 gas (3×10^4 or 1×10^5 Pa) at 200, 300 and 400 °C for 3, 10, 20 or 30 min. The amount of natural graphite was 300 mg for one batch reaction. Surface composition of surface-chlorinated samples was determined by X-ray photoelectron spectroscopy (XPS) (SHIMADZU, ESCA-3400 with Mg Ká radiation). Surface disorder and its effect to the bulk structure were evaluated by Raman spectroscopy (Ranishaw inVia Raman Microscope, 532 nm) and X-ray diffractometry (SHIMADZU, XRD-6100), respectively.

2. 2. Electrochemical Measurements for Surface-chlorinated Natural Graphite Samples

Beaker type three electrode-cell with natural graphite sample as a working electrode and metallic lithium as counter and reference electrodes was used for galvanostatic charge/discharge experiments. Electrolyte solutions were 1 $molL^{-1}$ $LiClO_4$ – EC/DEC/PC (1:1:1 vol.) (Kishida Chemicals, Co. Ltd., H_2O: 2–10 ppm) and 1 $molL^{-1}$ $LiPF_6$–EC/EMC/PC (1:1:1 vol.) (Kishida Chemicals, Co. Ltd., H_2O: ≤ 3 ppm). Natural graphite electrode was prepared as follows. Natural graphite powder sample was dispersed in N-methyl-2-pyrrolidone (NMP) containing 12 wt% poly(vinylidene fluoride) (PVdF) and slurry was pasted on a copper current collector. The electrode was dried at 120 °C under vacuum attained by a rotary pump for half a day. After drying, the electrode contained 80 wt% natural graphite sample and 20 wt% PVdF. Charge/discharge experiments were performed at a current density of 60 mAg^{-1} or 300 mAg^{-1} between 0 and 3 V relative to Li/Li^+ reference electrode at 25 °C.

3. Results and Discussion

3. 1. Surface Composition and Structure of Chlorinated Natural Graphite Samples

Surface composition and XPS spectra of chlorinated natural graphite samples are shown in Table 1 and Figs. 1 and 2, respectively. Small amounts of surface chlorine were detected for NG10 μm chlorinated by Cl_2 of 1×10^5 Pa at 400 °C for 10–30 min and NG15 μm chlorinated by Cl_2 of 1×10^5 Pa at 400 °C for 20 and 30 min while only a trace of chlorine was detected for all other samples as shown in Table 1. The surface-chlorinated samples are stable in air and under high vacuum during XPS measurement. Chlorination of active carbon by Cl_2 at 550–600 °C gives hydrophobic chlorinated material.[59] This means that high temperature reaction of Cl_2 with carbon materials gives covalent C–Cl bonds. However, only the surface is chlorinated in the case of graphite with high crystallinity. It is known that chlorine is not intercalated in graphite. The Cl $2p_{3/2}$ and Cl $2p_{1/2}$ peaks are observed at 198.6 and 200.1 eV, respectively. These binding energies are not large values. The reason may be that surface-chlorinated sample is electro-conductive because covalent C–Cl and C=O bonds partly cover the graphite surface as discussed later. The surface chlorine was obviously lower than surface fluorine detected for NG10 μm and NG15 μm fluorinated under mild conditions (F_2: 3×10^4 Pa, temp.: 200 and 300 °C, time: 2 min).[47,49] Surface chlorine concentrations were only 0.1–0.2 at% when NG10 μm and NG15 μm were chlorinated with 3×10^4 Pa Cl_2, at 200 and 300 °C and for 3 min. They were 0.2–0.3 at% even under the conditions of 1×10^5 Pa Cl_2, 300 °C and 10 min. To obtain 0.5 at% or higher surface chlorine concentrations, chlorination conditions such as 1×10^5 Pa Cl_2, 400 °C and 10–30 min are necessary as given in Table 1. Surface fluorine concentrations of the same NG10 μm and NG15 μm were 11–20 at% under the fluorination conditions, 3×10^4 Pa F_2, 200 and 300 °C, and 2 min,[47,49] which are much weaker reaction conditions than in the case of surface chlorination with Cl_2. Nevertheless the surface fluorine concentrations are much larger than surface chlorine concentrations obtained in the present study. Main reasons are the difference in the reactivity between F_2 and Cl_2 gases and electronegativities of fluorine and chlorine. On the other hand, surface oxygen concentrations slightly increased compa-

Table 1 Surface composition of chlorinated natural graphite samples.

Sample	Chlorination			NG10 μm			NG15 μm		
	Cl_2 (Pa)	Temp. (°C)	Time (min)	C	Cl	O	C	Cl	O
				(at%)					
Original	–	–	–	92.8	–	7.2	93.3	–	6.7
A, a	3×10^4	200	3	86.3	0.1	13.6	90.4	0.2	9.4
B, b	3×10^4	300	3	89.8	0.1	10.1	88.5	0.2	11.3
C, c	1×10^5	300	10	90.4	0.2	9.3	90.0	0.3	9.7
D, d	1×10^5	400	10	88.6	0.5	10.9	90.4	0.3	9.3
E, e	1×10^5	400	20	91.1	0.9	8.0	90.6	0.7	8.7
F, f	1×10^5	400	30	90.1	1.4	8.5	85.8	2.3	11.9

A–F: surface-chlorinated NG10 μm; a–f: surface-chlorinated NG15 μm.

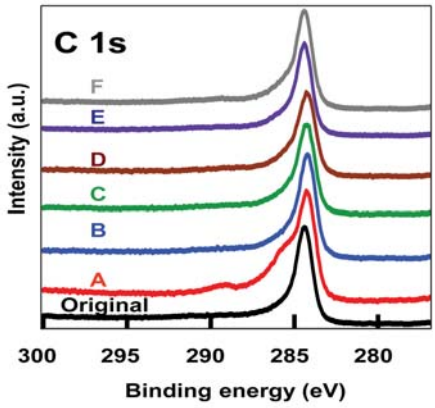

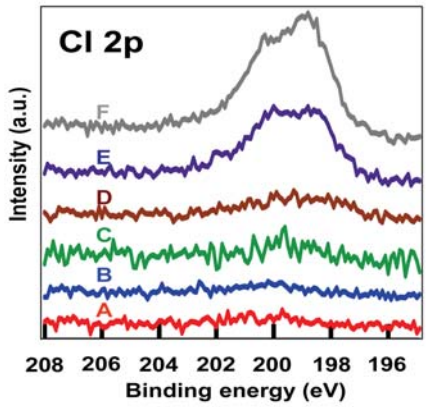

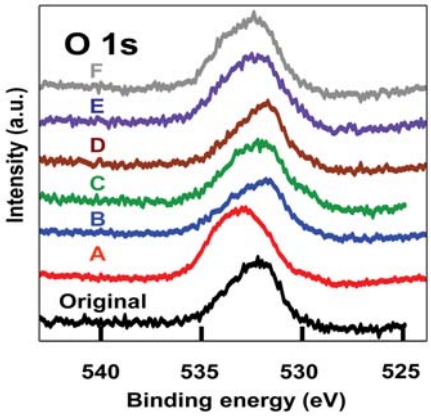

Fig. 1. XPS spectra of original and surface-chlorinated NG10 μm samples. (Chlorination conditions of samples A–F are given in Table 1.)

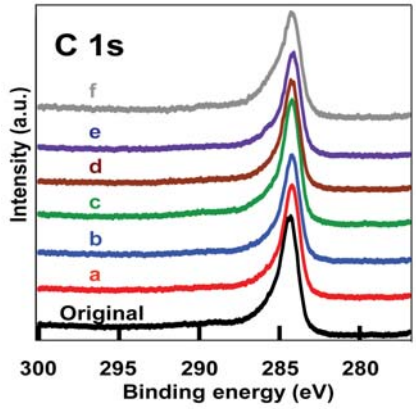

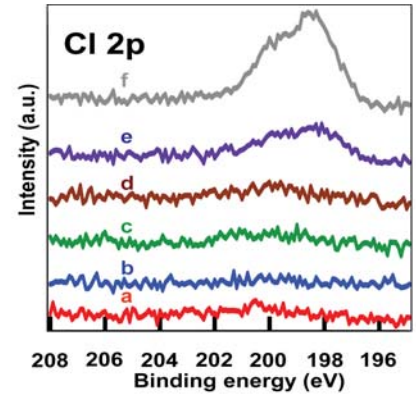

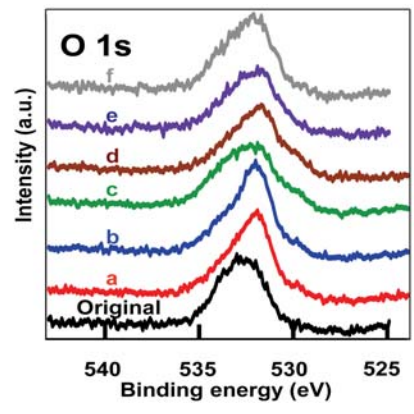

Fig. 2. XPS spectra of original and surface-chlorinated NG15 μm samples. (Chlorination conditions of samples a–f are given in Table 1.)

red with those of original NG10 μm and NG15 μm particularly under mild chlorination conditions (3×10^4 Pa Cl_2, 200 and 300 °C, 3 min and 1×10^5 Pa Cl_2, 300 °C, 10 min). They were reduced in the case of surface fluorination with F_2,[47,49] which is probably because some amount of surface oxygen is removed as COF_2 gas by breaking of C–C bond. When Cl_2 gas is introduced into Ni reactor, it reacts with adsorbed water molecules, yielding unstable HClO ($Cl_2 + H_2O \rightarrow HClO + HCl$). Complete removal of adsorbed water is normally difficult because the temperature in the vicinity of flange of the reactor is lower than the chlorination temperatures. The reactions of lattice defects with HClO and HClO+Cl_2 may give >C=O and -C=O(Cl) groups, respectively (>C + HClO → >C=O + HCl and -C + HClO + 1/2Cl_2 → –C=O(Cl) + HCl). This would be the reason why surface oxygen concentrations were increased by chlorination. It is also inferred that unstable HClO causes the formation of surface lattice defects by breaking C–C bonds and releasing oxygen as CO gas. Under stronger chlorination conditions (1×10^5 Pa Cl_2, 400 °C, 10–30 min), surface chlorine concentrations increased to 0.5–2.3 at% and surface oxygen slightly decreased, which suggest that formation of –CCl_3 and >CCl_2 groups preferentially takes place by the reactions of Cl_2 with surface lattice defects (-C + 3/2Cl_2 → –CCl_3, >C + Cl_2 → >CCl_2).

The d_{002} values were not changed by chlorination, being 0.335–0.336 nm for original and surface-chlorinated samples. Half widths of (002) X-ray diffraction lines only slightly broadened by chlorination. Raman spectroscopy also revealed almost no change of surface structural disorder by chlorination as shown in Fig. 3. G-band and D-band appear at 1580 and 1360 cm^{-1}, indicating graphitic and disordered structures of carbon materials. The ratios of D-band to G-band intensity ($R=I_D/I_G$) showing the degree of surface disorder were 0.35 and 0.39 for original NG10 μm and NG15 μm, respectively. The R values were 0.33–0.39 and 0.35–0.37 for surface-chlorinated NG10 μm and NG15 μm samples, respectively, which indicates that surface disorder of NG10 μm and NG15 μm is nearly the same before and after chlorination. This is another difference from the fluorination accompanying the increase in surface disorder.[47, 49]

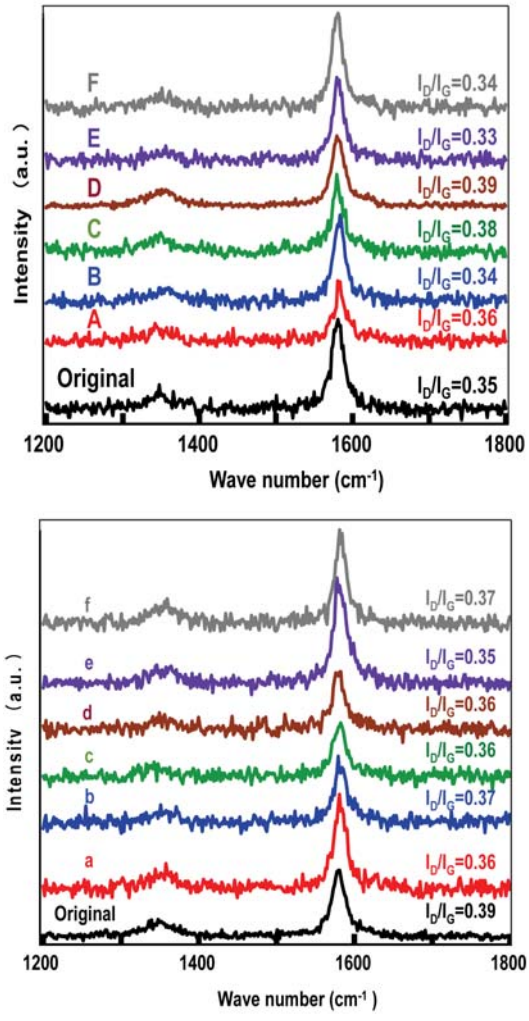

Fig. 3. Raman spectra of original and surface-chlorinated natural graphite samples. (Chlorination conditions of samples A–F (NG10 μm) and a–f (NG15 μm) are given in Table 1.)

3. 2. Charge/discharge Behavior of Surface-chlorinated Natural Graphite Samples

Fig. 4 shows charge/discharge potential curves at 1st cycle, obtained in 1 $molL^{-1}$ $LiClO_4$–EC/DEC/PC (1:1:1 vol.) at 60 mAg^{-1}. NG10 μm gave the higher first coulombic efficiency (58.9%) than NG15 μm (49.5%). The surface areas of NG10 μm and NG15 μm are 9.2 and 6.9 m^2g^{-1}, respectively.[47] Since charge/discharge experiments were made by constant current method at 60 mAg^{-1}, actual current density is the higher in NG15 μm than NG10 μm. This would be the reason why NG10 μm has a higher first coulombic efficiency than NG15 μm. The potential plateaus at 0.8 V vs Li/Li^+ indicate reductive decomposition of PC. The surface >C=O and -C=O(Cl) groups which would be formed by chlorination should contribute to the decrease in surface lattice defects together with -CCl_3 and >CCl_2 groups. However, first coulombic efficiencies were low for the samples, A–B and a–d chlorinated under mild conditions. This may be due to that unstable HClO simultaneously yields surface lattice defects by C–C bond breaking. In addition, surface oxygen concentrations increased under mild chlorination conditions and slightly decreased under stronger conditions (1×10^5 Pa Cl_2, 400 °C, 10–30 min), which suggests that formation of surface lattice defects by the reaction of HClO with natural graphite decreases and covalent C–Cl bonds are preferentially formed under the stronger chlorination conditions. First coulombic efficiency for NG10 μm increased from 58.9% to 81.0% with increasing surface chlorine (Table 2). Particu-

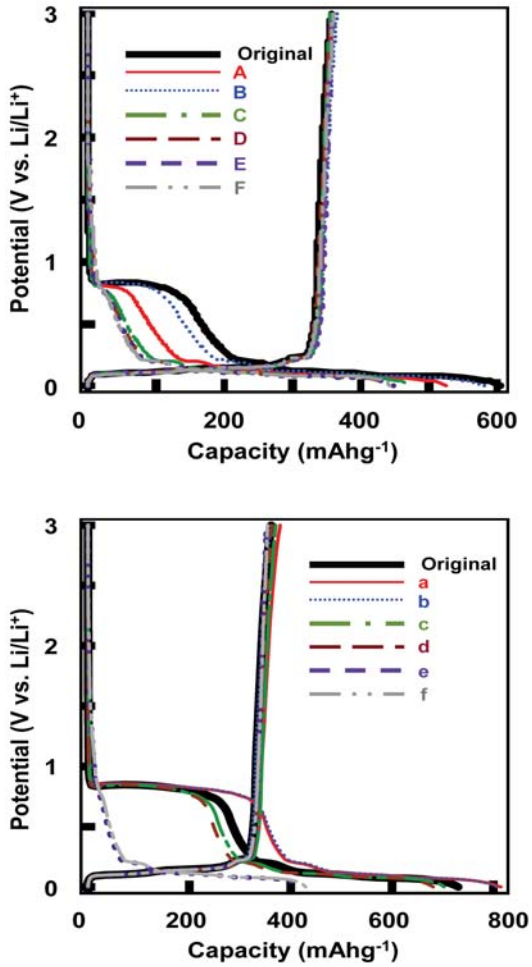

Fig. 4. First charge/discharge potential curves of original and surface-chlorinated natural graphite samples at 60 mAg^{-1} in 1 $molL^{-1}$ $LiClO_4$–EC/DEC/PC (1:1:1 vol.). (Chlorination conditions of samples A–F (NG10 μm) and a–f (NG15 μm) are given in Table 1.)

Table 2. Charge/discharge capacities and coulombic efficiencies for original and surface-chlorinated NG10 μm samples at 1st cycle, obtained in 1 $molL^{-1}$ $LiClO_4$–EC/DEC/PC (1:1:1 vol.) at 60 mAg^{-1}. (Chlorination conditions of samples A–F are given in Table 1.)

Graphite sample	Discharge capacity ($mAhg^{-1}$)	Charge capacity ($mAhg^{-1}$)	Coulombic efficiency (%)
Original	605	357	58.9
A	526	359	68.2
B	585	365	62.4
C	472	356	75.4
D	447	356	79.5
E	449	359	79.8
F	444	359	81.0

Table 3. Charge/discharge capacities and coulombic efficiencies for original and surface-chlorinated NG15 μm samples at 1st cycle, obtained in 1 $molL^{-1}$ $LiClO_4$–EC/DEC/PC (1:1:1 vol.) at 60 mAg^{-1}. (Chlorination conditions of samples a–f are given in Table 1.)

Graphite sample	Discharge capacity ($mAhg^{-1}$)	Charge capacity ($mAhg^{-1}$)	Coulombic efficiency (%)
Original	731	361	49.5
a	798	364	45.6
b	807	361	44.7
c	703	371	52.7
d	681	363	53.3
e	427	352	82.4
f	430	354	82.4

larly samples D, E and F with relatively larger surface chlorine concentrations of 0.5–1.4 at% gave high first coulombic efficiencies (79.5–81.0%). In the case of NG15 μm, first coulombic efficiency of original sample was 49.5% which is lower than that of NG10 μm by 10%. The samples e and f with surface chlorine concentrations of 0.7 and 2.3 at%, respectively, exhibited high first coulombic efficiencies of 82.4% (Table 3). First coulombic efficiencies thus increased with increasing surface chlorine and also oxygen concentrations. This result suggests that surface lattice defects acting as active sites for PC decomposition are reduced by the formation of covalent C–Cl bonds (-CCl_3 and >CCl_2 groups) and also C=O bonds (>C=O and -C=O(Cl) groups). First charge capacities of all NG10 μm and NG15 μm samples were 350–360 $mAhg^{-1}$ as given in Tables 2 and 3, and cycleability was also good.

On the other hand, the results are somewhat different in 1 $molL^{-1}$ $LiPF_6$–EC/EMC/PC (1:1:1 vol.). First coulombic efficiencies for non-chlorinated NG10 μm and NG15 μm were both higher in 1 $molL^{-1}$ $LiPF_6$–EC/EMC/PC (1:1:1 vol.) than in 1 $molL^{-1}$ $LiClO_4$–EC/DEC/PC (1:1:1 vol.), being 75.0 and 63.8% at 60 mAg^{-1}, and 66.4 and 58.3% at 300 mAg^{-1}, respectively (Figs. 5 and 6, and Table 4). The first coulombic efficiencies for original NG10 μm and NG15 μm are higher by 14–16% in 1 $molL^{-1}$ $LiPF_6$–EC/EMC/PC (1:1:1 vol.) than in 1 $molL^{-1}$ $LiClO_4$–EC/DEC/PC (1:1:1 vol.). This is probably because a small amount of LiF generated by the reaction of $LiPF_6$ with Li facilitates the formation of surface film on graphite. The electrode potentials more quicky decreased in surface-chlorinated samples than original graphite in the case of NG15 μm as shown in Figs. 5 and 6. However, potential profiles are similar to each other for original and surface-chlorinated NG10 μm samples. Table 4 shows that the larger increase in the first coulombic efficiencies is observed for NG15 μm having the smaller surface area than NG10 μm, and at the higher current density of 300 mAg^{-1} than 60 mAg^{-1}. The increments of first coulombic efficiencies for NG15 μm reached ~15% and ~18% at 60 and 300 mAg^{-1}, respectively. In the case of NG10 μm, the increments of first coulombic efficiencies were ~8% even at 300 mAg^{-1}. The results show that the

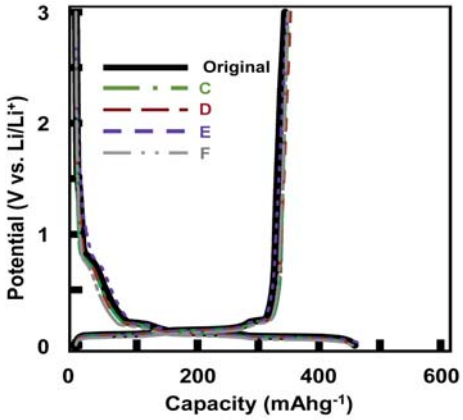

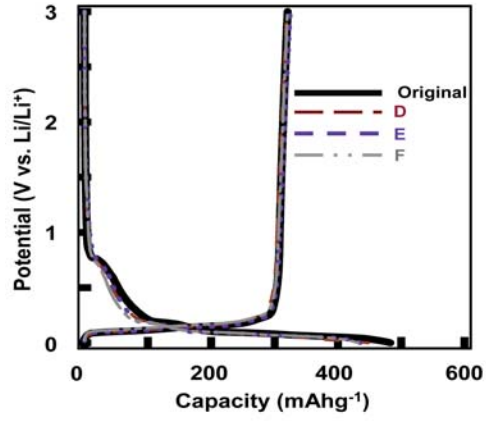

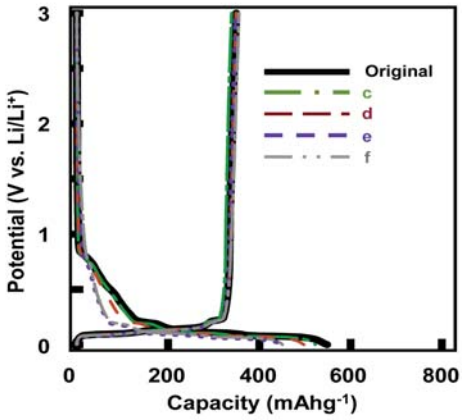

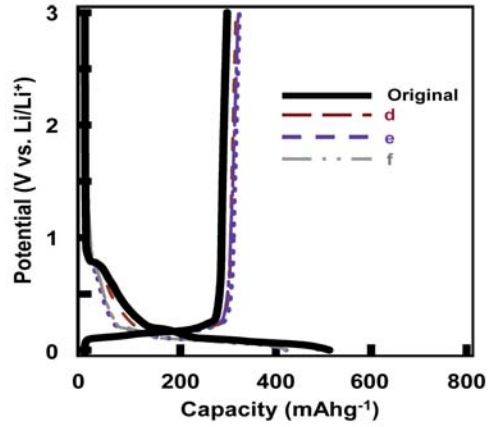

Fig. 5. First charge/discharge potential curves of original and surface-chlorinated natural graphite samples at 60 mAg^{-1} in 1 $molL^{-1}$ $LiPF_6$–EC/EMC/PC (1:1:1 vol.). (Chlorination conditions of samples C–F (NG10 μm) and c–f (NG15 μm) are given in Table 1.)

Fig. 6. First charge/discharge potential curves of original and surface-chlorinated natural graphite samples at 300 mAg^{-1} in 1 $molL^{-1}$ $LiPF_6$–EC/EMC/PC (1:1:1 vol.). (Chlorination conditions of samples D–F (NG10 μm) and d–f (NG15 μm) are given in Table 1.)

Table 4 First coulombic efficiencies for original and surface-chlorinated NG10 μm and NG15 μm samples in 1 $molL^{-1}$ $LiPF_6$–EC/EMC/PC (1:1:1 vol.) at 60 and 300 mAg^{-1}. (Chlorination conditions of samples C–F and c–f are given in Table 1.)

Sample	60 mAg^{-1}	300 mAg^{-1}	Sample	60 mAg^{-1}	300 mAg^{-1}
NG10 μm	75.0	66.4 (%)	NG15 μm	63.8	58.3 (%)
C	76.8	–	c	64.9	–
D	78.0	71.3	d	70.1	64.7
E	74.0	74.6	e	77.2	76.7
F	77.0	74.2	f	78.9	76.3

effect of surface chlorination on first coulombic efficiency appears at a high current density in $LiPF_6$–containing electrolyte solution. As mentioned in the introduction, the reactivity and electronegativity of Cl_2 are lower than those of F_2. Therefore the stronger reaction conditions are necessary for the formation of covalent C–Cl bonds. Chlorination also causes the formation of covalent C=O bonds which would contribute to the decrease in surface lattice defects. In conclusion, surface chlorination is a good method for surface passivation of natural graphite powder to use natural graphite electrode in PC-containing electrolyte solution.

4. Conclusions

It is difficult to use PC-containing electrolyte solution for natural graphite powder electrode since PC is easily reduced on natural graphite, which largely increases irreversible capacity, i.e. decreasing first coulombic efficiency. This would be because surface lattice defects of natural graphite powder act as active sites for electrochemical reduction of PC. To improve charge/discharge characteristics of natural graphite powder electrode in PC-containing electrolyte solution, surface chlorination of natural graphite powder has been performed to passivate the surface active sites. Chlorination of natural graphite pow-

der increases both surface chlorine and oxygen concentrations. Both surface chlorine and oxygen would contribute to the decrease in surface lattice defects by the formation of covalent C–Cl and C=O bonds. Surface-chlorinated natural graphite samples having 0.5–2.3 at% Cl well suppress the electrochemical decomposition of PC, increasing first coulombic efficiencies by 20–30% in 1 $molL^{-1}$ $LiClO_4$–EC/DEC/PC (1:1:1 vol.). In 1 $molL^{-1}$ $LiPF_6$–EC/EMC/PC (1:1:1 vol.), the effect of surface chlorination is observed at a higher current density. The increments of first coulombic efficiencies for NG15 μm with smaller surface reached ~15% and ~18% at 60 and 300 mAg^{-1}, respectively. These results were obtained under the chlorination conditions of 1×10^5 Pa Cl_2, 400°C and 10–30 min.

5. Acknowledgements

The present study was partly supported by Ministry of Education, Culture, Sports, Science and Technology (MEXT) Private University Project Grant under Contract # S1001033. Natural graphite used in the study was kindly supplied by SEC Carbon Co., Ltd. The authors gratefully acknowledge them.

6. References

1. H. Wang, M. Yoshio, *J. Power Sources* **2001**, *93*, 123–129.
2. S. Soon, H. Kim, S. M. Oh, *J. Power Sources* **2001**, *94*, 68–73.
3. M. Yoshio, H. Wang, K. Fukuda, Y. Hara, Y. Adachi, *J. Electrochem. Soc.* **2000**, *147*, 1245–1250.
4. H. Wang, M. Yoshio, T. Abe, Z. Ogumi, *J. Electrochem. Soc.* **2002**, *149*, A499–A503.
5. M. Yoshio, H. Wang, K. Fukuda, T. Umeno, N. Dimov, Z. Ogumi, *J. Electrochem. Soc.* **2002**, *149*, A1598–A1603.
6. Y.-S. Han, J.-Y. Lee, *Electrochim. Acta* **2003**, *48*, 1073–1079.
7. Y. Ohzawa, M. Mitani, T. Suzuki, V. Gupta, T. Nakajima, *J. Power Sources* **2003**, *122*, 153–161.
8. Y. Ohzawa, Y. Yamanaka, K. Naga, T. Nakajima, *J. Power Sources* **2005**, *146*, 125–128.
9. Y. Ohzawa, T. Suzuki, T. Achiha, T. Nakajima, *J. Phys. Chem. Solids* **2010**, *71*, 654–657.
10. H.-Y. Lee, J.-K. Baek, S.-M. Lee, H.-K. Park, K.-Y. Lee, M.-H. kim, *J. Power Sources* **2004**, *128*, 61–66.
11. W.-H. Zhang, I. Fang, M. Yue, Z.-L. Yu, *J. Power Sources* **2007**, *174*, 766–769.
12. J.-H. Lee, H.-Y. Lee, S.-M. Oh, S.-J. Lee, K.-Y. Lee, S.-M. lee, *J. Power Sources* **2007**, *166*, 250–254.
13. Y.-S. Park, H. J. Bang, S.-M. Oh, Y.-K. Sun, S.-M. Lee, *J. Power Sources* **2009**, *190*, 553–557.
14. G. Park, N. Gunawardhana, H. Nakamura, Y.-S. Lee, M. Yoshio, *J. Power Sources* **2011**, *196*, 9820–9824.
15. R. Takagi, T. Okubo, K. Sekine, T. Takamura, *Electrochemistry* **1997**, *65*, 333–334.
16. T. Takamura, K. Sumiya, J. Suzuki, C. Yamada, K. Sekine, *J. Power Sources* **1999**, *81/82*, 368–372.
17. Y. Wu, C. Jiang, C. Wan, E. Tsuchida, *Electrochem. Commun.* **2000**, *2*, 626–629.
18. S.-S. Kim, Y. Kadoma, H. Ikuta, Y. Uchimoto, M. Wakihara, *Electrochem. Solid-State Lett.* **2001**, *4*, A109–A112.
19. J. K. Lee, D. H. Ryu, J. B. Ju, Y. G. Shul, B. W. Cho, D. Park, *J. Power Sources* **2002**, *107*, 90–97.
20. I. R. M. Kottegoda, Y. Kadoma, H. Ikuta, Y. Uchimoto, M. Wakihara, *Electrochem. Solid-State Lett.* **2002**, *5*, A275–A278.
21. I. R. M. Kottegoda, Y. Kadoma, H. Ikuta, Y. Uchimoto, M. Wakihara, *J. Electrochem. Soc.* **2005**, *152*, A1595–A1599.
22. L. J. Fu, J. Gao, T. Zhang, Q. Cao, L. C. Yang, Y. P. Wu, R. Holze, *J. Power Sources* **2007**, *171*, 904–907.
23. F. Nobili, S. Dsoke, M. Mancini, R. Tossici, R. Marassi, *J. Power Sources* **2008**, *180*, 845–851.
24. M. Mancini, F. Nobili, S. Dsoke, F. D'Amico, R. Tossici, F. Croce, R. Marassi, *J. Power Sources* **2009**, *190*, 141–148.
25. F. Nobili, M. Mancini, P. E. Stallworth, F. Croce, S. G. greenbaum, R. Marassi, *J. Power Sources* **2012**, *198*, 243–250.
26. E. Peled, C. Menachem, D. Bar-Tow, A. Melman, *J. Electrochem. Soc.* **1996**, *143*, L4–L7.
27. J. S. Xue, J. R. Dahn, *J. Electrochem. Soc.* **1995**, *142*, 3668–3677.
28. Y. Ein-Eli, V. R. Koch, *J. Electrochem. Soc.* **1997**, *144*, 2968–2973.
29. Y. Wu, C. Jiang, C. Wan, E. Tsuchida, *J. Mater. Chem.* **2001**, *11*, 1233–1236.
30. Y. P. Wu, C. Jiang, C. Wan, R. Holze, *Electrochem. Commun.* **2002**, *4*, 483–487.
31. Y. Wu, C. Jiang, C. Wan, R. Holze, *J. Power Sources* **2002**, *111*, 329–334.
32. Y. P. Wu, C. Jiang, C. Wan, R. Holze, *J. Appl. Electrochem.* **2002**, *32*, 1011–1017.
33. J. Shim, K. A. Striebel, *J. Power Sources* **2007**, *164*, 862–867.
34. T. Nakajima, M. Koh, R.N. Singh, M. Shimada, *Electrochim. Acta* **1999**, *44*, 2879–2888.
35. V. Gupta, T. Nakajima, Y. Ohzawa, H. Iwata, *J. Fluorine Chem.* **2001**, *112*, 233–240.
36. T. Nakajima, V. Gupta, Y. Ohzawa, H. Iwata, A. Tressaud, E. Durand, *J. Fluorine Chem.* **2002**, *114*, 209–214.
37. T. Nakajima, V. Gupta, Y. Ohzawa, M. Koh, R.N. Singh, A. Tressaud, E. Durand, *J. Power Sources* **2002**, *104*, 108–114.
38. T. Nakajima, J. Li, K. Naga, K. Yoneshima, T. Nakai, Y. Ohzawa, *J. Power Sources* **2004**, *133*, 243–251.
39. J. Li, K. Naga, Y. Ohzawa, T. Nakajima, A. P. Shames, A. I. Panich, *J. Fluorine Chem.* **2005**, *126*, 265–273.
40. J. Li, Y. Ohzawa, T. Nakajima, H. Iwata, *J. Fluorine Chem.* **2005**, *126*, 1028–1035.
41. H. Groult, T. Nakajima, L. Perrigaud, Y. Ohzawa, H. Yashiro, S. Komaba, N. Kumagai, *J. Fluorine Chem.* **2005**, *126*, 1111–1116.
42. K. Matsumoto, J. Li, Y. Ohzawa, T. Nakajima, Z. Mazej, B. Žemva, *J. Fluorine Chem.* **2006**, *127*, 1383–1389.

43. K. Naga, T. Nakajima, Y. Ohzawa, B. Žemva, Z. Mazej, H. Groult, *J. Electrochem. Soc.* **2007**, *154*, A347–A352.
44. K. Naga, T. Nakajima, S. Aimura, Y. Ohzawa, B. Žemva, Z. Mazej, H. Groult, A. Yoshida, *J. Power Sources* **2007**, *167*, 192–199.
45. T. Nakajima, S. Shibata, K. Naga, Y. Ohzawa, A. Tressaud, E. Durand, H. Groult, F. Warmont, *J. Powerr Sources* **2007**, *168*, 265–271.
46. H. Groult, T. Nakajima, A. Tressaud, S. Shibata, E. Durand, L. Perrigaud, F. Warmont, *Electrochem. Solid-State Lett*. **2007**, *10*, A212–A215.
47. T. Achiha, T. Nakajima, Y. Ohzawa, *J. Electrochem. Soc.* **2007**, *154*, A827–A833.
48. T. Achiha, S. Shibata, T. Nakajima, Y. Ohzawa, A. Tressaud, E. Durand, *J. Power Sources* **2007**, *171*, 932–937.
49. T. Nakajima, T. Achiha, Y. Ohzawa, A. M. Panich, A. I. Shames, *J. Phys. Chem. Solids* **2008**, *69*, 1292–1295.
50. X. Cheng, J. Li, T. Achiha, T. Nakajima, Y. Ohzawa, Z. Mazej, B. Žemva, *J. Electrochem. Soc.* **2008**, *155*, A405–A413.
51. S. Kuwabata, N. Tsumura, S. Goda, C. R. Martin, H. Yoneyama, *J. Electrochem. Soc.* **1998**, *145*, 1415–1420.
52. M. Gaberscek, M. Bele, J. Drofenik, R. Dominko, S. Pejovnik, *Electrochem. Solid State Lett.* **2000**, *3*, 171–173.
53. J. Drofenik, M. Gaberscek, R. Dominko, M. Bele, S. Pejovnik, *J. Power Sources* **2001**, *94*, 97–101.
54. M. Bele, M. Gaberscek, R. Dominko, J. Drofenik, K. Zupan, P. Komac, K. Kocevar, I. Musevic, S. Pejovnik, *Carbon* **2002**, *40*, 1117–1122.
55. M. Gaberscek, M. Bele, J. Drofenik, R. Dominko, S. Pejovnik, *J. Power Sources* **2001**, *97/98*, 67–69.
56. B. Veeraraghavan, J. Paul, B. Haran, B. Popov, *J. Power Sources* **2002**, *109*, 377–387.
57. M. Holzapfel, H. Buqa, F. Krumeich, P. Novak, F. M. Petrat, C. Veit, *Electrochem. Solid-State Lett.* **2005**, *8*, A516–A520.
58. C.-C. Chang, *J. Power Sources* **2008**, *175*, 874–880.
59. Y. Kanaya, N. Watanabe, *DENKI KAGAKU* **1974**, *42*, 349–353.

Povzetek

Površinske nepravilnosti kristalinične snovi lahko delujejo kot aktivna mesta za elektrokemijsko redukcijo propilen karbonata (PC), ki se uporablja kot topilo v litij-ionskih baterijah. Učinek površinskega kloriranja naravnega grafita v prahu je bil predmet raziskave z namenom izboljšanja karakteristik grafitnih elektrod v elektrolitskih raztopinah, ki vsebujejo propilen karbonat. S kloriranjem naravnega grafita se poveča ne le vsebnost površinsko vezanega klora ampak tudi kisika. Oboje prispeva k zmanjšanju površinske nepravilnosti naravnega grafita. Pri vzorcih pripravljenih s površinskim kloriranjem naravnega grafita s koncentracijo klora med 0,5–2,3 % se je občutno zmanjšal elektrokemijski razpad propilen karbonata, zmanjša se ireverzibilna kapaciteta oziroma v 1 mol raztopini $LiClO_4$ v EC/DEC/PC (1:1:1 vol. deleži) se poveča Coulombova učinkovitost pri prvem polnjenju za 20–30%. V primeru 1 mol raztopine $LiPF_6$ v EC/EMC/PC (1:1:1 vol. deleži) opazimo efekt površinskega kloriranja pri večji gostoti toka. To lahko pripišemo zmanjšanju nepravilnosti na površini naravnega grafita zaradi nastanka kovalentnih C–Cl in C=O vezi.